Magnetic structure of $La_{0.7}Sr_{0.3}MnO_3/La_{0.7}Sr_{0.3}FeO_3$ superlattices*

E. Arenholz,[1] G. van der Laan,[2] F. Yang,[3] N. Kemik,[3]

M. D. Biegalski,[4] H. M. Christen,[4] and Y. Takamura[3]

[1]*Advanced Light Source, Lawrence Berkeley National Laboratory, Berkeley, CA 94720, USA*

[2]*Diamond Light Source, Chilton, Didcot,*

Oxfordshire OX11 0DE, United Kingdom

[3]*Department of Chemical Engineering and Materials Science, UC Davis, CA 95616, USA*

[4]*Center for Nanophase Materials Science,*

Oak Ridge National Laboratory, Oak Ridge, TN 37831, USA

(Dated: January 29, 2009)

Abstract

Using x-ray magnetic dichroism we characterize the magnetic order in $La_{0.7}Sr_{0.3}MnO_3$ (LSMO) / $La_{0.7}Sr_{0.3}FeO_3$ (LSFO) superlattices with 6 unit cell thick sublayers. The LSMO layers exhibit a reduced Curie temperature compared to the bulk while antiferromagnetic order in the LSFO layers persists up to the bulk Neél temperature. Moreover, we find that aligning the LSMO magnetization by a magnetic field within the (001) surface plane leads to a reorientation of the Fe moments as well maintaining a perpendicular orientation of Fe and Mn moments. This perpendicular alignment is due to the frustrated exchange coupling at the LSMO/LSFO interface.

PACS numbers: 75.70.Ak, 75.70.Cn , 78.70.Dm, 78.20.Bh

*This work was supported by the U.S. Department of Energy under Contract No. DE-AC02-05CH11231.

The combination of unique magnetic characteristics induced by reduced dimensionality and strong magnetic interactions across interfaces can lead to intriguing properties in magnetic bilayers and superlattices not observed in the constituent materials in bulk form. For instance, epitaxial strain induces a perpendicular magnetic anisotropy in Ni thin films grown on Cu(001) [1] but deposition of three monolayers of Co with a preferential in-plane orientation of the moments forces the Ni moments into the surface plane [2] due to the strong exchange interaction through the Co/Ni interface. Another example is cooling a ferromagnetic (FM)/ antiferromagnetic (AFM) bilayer in an external magnetic field through the Néel temperature of the antiferromagnet causing a shift in the FM hysteresis loop away from zero field. The magnitude and sign of the loop shift, called exchange bias, depend strongly on the exact interface structure, e.g., the presence of uncompensated moments [3] and roughness at the interface [4] as well as the properties of the individual layers [5]. It is the careful optimization of the characteristics of the individual layers as well as the magnetic coupling across the interface that allows us to control the magnetic properties of superlattices and tailor them for devices, e.g., in information storage and processing technology.

In this paper we determine the magnetic structure of $La_{0.7}Sr_{0.3}MnO_3$ (LSMO)/$La_{0.7}Sr_{0.3}FeO_3$ (LSFO) superlattices with 6 unit cell thick sublayers using a combination of x-ray magnetic circular dichroism (XMCD) and x-ray magnetic linear dichroism (XMLD). The experiments show that the Mn and Fe moments are aligned perpendicularly up to the Curie temperature of the LSMO sublayers for any inplane orientation of the LSMO magnetization. This behavior is due to the frustrated exchange coupling at the interface and the weak anisotropy in the LSFO layer. AFM order in the LSFO layer persists up to temperatures exceeding 400 K while the LSMO FM order disappears around 200 K.

LSMO and LSFO both have perovskite structures, i.e., the La^{3+} and Sr^{2+} cations are arranged in a simple cubic array with M^{3+} and M^{4+} (M = Mn, Fe) cations at the body center and O^{2-} ions at the face centered positions, forming MO_6 octahedra. Bulk LSMO exhibits a Curie temperature, T_C, of 360 K [6] while the AFM insulator LSFO has a Néel temperature between 300 and 420 K [7].

LSMO/LSFO superlattices were grown on $SrTiO_3$(001) substrates by pulsed laser deposition using a KrF laser operated at 10 Hz and a fluence 1.2 J cm^{-2}. The same La:Sr ratio of 2:1 was chosen for the LSMO and LSFO sublayers to prevent Sr diffusion near the interfaces.

During growth, the substrate was held at 973 K in an oxygen background pressure of 0.2 torr and cooled after deposition in an oxygen pressure of 300 torr to assure proper film oxygenation. In situ reflection high energy electron diffraction (RHEED) indicated layer-by-layer growth and allowed precise control of the sublayer thicknesses. Ex-situ x-ray diffraction measurements confirmed the correct periodicity of the superlattices and indicated a high crystalline quality. In thin film form deposited on $SrTiO_3(001)$, the LSMO and LSFO crystal lattices can be approximated by using the same crystallographic notation as the cubic $SrTiO_3$ substrate ($a = 3.905$ Å). Due to the lattice mismatch (0.64%) the epitaxial LSMO film ($a = 3.87$ Å) distorts tetragonally. The preferred LSFO orientation results in a nearly perfect lattice match between LSFO and $SrTiO_3$ ($a = 3.905$ Å). The thickness dependence of the structural and magnetotransport properties as well as magnetometry results will be discussed elsewhere [8]. Here we focus on a detailed study of the magnetic characteristics of the LSMO/LSFO superlattice with 6 unit cell thick sublayers using soft x-ray dichroism.

X-ray absorption (XA) spectra were measured using an eight-pole resistive electromagnet [9] on beamline 4.0.2 at the Advanced Light Source (ALS) in total-electron-yield mode by monitoring the sample drain current. XMCD spectra were acquired in an applied field of 0.3 T collinear with the x-ray beam which impinged on the sample surface at 60° to the sample normal. At 50 K a strong XMCD signal is observed at the Mn $L_{2,3}$ edges (not shown). Its spectral shape and magnitude is in good agreement with previous reports on bulk LSMO [10]. No XMCD is observed at the Fe $L_{2,3}$ edges as expected for AFM LSFO, also indicating that no uncompensated Fe moments are present near the LSMO/LSFO interface.

To determine the LSMO/LSFO interfacial coupling and to evaluate the impact of the magnetization reversal in the LSMO layer on the LSFO magnetic structure, we monitored in normal incidence geometry the Fe $L_{2,3}$ XMLD obtained as the difference between XA spectra with **H** perpendicular and parallel to **E**. An external field of 0.3 T is applied to align the Mn moments parallel or perpendicular to the x-ray polarization which in turn is oriented parallel ($\phi = 0°$) or at $\phi = 45°$ to the [100] direction within in the (001) surface plane. The experimental geometry is depicted in the inset of Fig. 1(a). To increase the electron-yield signal, the field was turned slightly out of the sample surface plane not appreciably effecting the spectral shape of the dichroism signals. Figure 1(a) shows the Fe $L_{2,3}$ XA spectrum obtained at 50 K and the XMLD spectra are shown in Fig. 1(b). The pronounced XMLD effect for both geometries indicates that when the magnetization of the LSMO layer is forced

by the magnetic field parallel or perpendicular to the x-ray polarization, a torque is created in the LSFO layer through exchange coupling realigning the Fe moments relative to the x-ray polarization as well. The strong angular dependence of the XMLD signal is caused by the influence of the crystalline electric field [11].

To distinguish between parallel and perpendicular alignment of the Mn and Fe moments, we performed atomic multiplet calculations [12] of the Fe $L_{2,3}$ XA and XMLD spectra [18] and a comparison with experimental data is shown in Fig. 1. All spectral features observed in the experiment are well reproduced by the calculation. From the spectra shown in Fig. 1(b) a perpendicular alignment of the Fe and Mn moments is derived, i.e. an external field along the [100] direction aligns the Mn moments with the in-plane [100] axis while the Fe moments are aligned along the in-plane [010] axis perpendicular to the field. The perpendicular alignment is a result of the frustrated exchange coupling between Mn moments in the ferromagnetic LSMO layer and the antiferromagnetically ordered Fe moments on the two sublattices in the LSFO layers. To minimize the energy, the moments in the FM LSMO and AFM LSFO layers align perpendicularly. This type of perpendicular alignment is expected for magnetically compensated antiferromagnetic plane at the interface to a ferromagnet [13].

Figure 2(a) shows the temperature dependence of the magnitude of the Mn $L_{2,3}$ XMCD signal. While the applied magnetic field renders the phase transition less distinct, it is possible to conclude that the Curie temperature of the LSMO layers is around 200 K while for of bulk LSMO 360 K has been reported [6]. However, the reduced layer thickness of 6 unit cells can be responsible for the reduced transition temperature [14]. Figure 2(a) also displays the temperature dependence of the Fe XMLD signal observed in the geometry of Fig. 1. This Fe XMLD effect resulting from the LSMO/LSFO exchange coupling tracks the magnitude of the Mn XMCD and vanishes at the transition temperature of the LSMO layer as expected

To obtain additional information about the magnetic order of the LSFO sublayer, the Fe $L_{2,3}$ XMLD temperature dependence was measured with the x-ray beam impinging on the sample surface at an angle of 60° to the sample normal. The x-ray polarization is oriented either parallel to the [010] axis in the (001) sample surface plane or close to the sample normal [001] as depicted in Fig. 2(b). An external field of 0.3 T was applied parallel to the x-ray beam leading to a collinear alignment of the Fe moments with the in-plane [010] axis for temperatures below the LSMO sublayer T_C. At 50 K, the linear dichroism spectrum derived

as difference between XA spectra obtained with in- and out-of-plane orientation of the x-ray polarization is within the experimental accuracy indistinguishable from I_0 shown in Fig. 1(b). This result suggests that the dichroism signal is dominated by the magnetic contribution in this temperature range and confirms that the Fe moments are oriented along the [010] in plane axis [15]. In the unstrained bulk LSFO lattice the [010] and [001] axes are equivalent and non-magnetic contributions to the linear dichroism signal are not expected. Even in the presence of a small lattice mismatch (0-1%) the resulting non-cubic linear dichroism is small [16] and cannot account for the linear dichroism observed here. The impact of epitaxial strain on the Fe $L_{2,3}$ XMLD signal will be discussed in detail elsewhere [17]. As shown in Fig. 2(b), the magnitude of the Fe XMLD tracks the Mn XMCD. At 200 K the Mn magnetization and hence the alignment of the Fe moments along the [010] axis vanishes and a domain pattern forms in the LSFO layers resulting in a reduced Fe XMLD signal. The Fe XMLD decreases in magnitude with increasing temperature but persists up to 400 K which is close to the bulk LSFO Neel temperature [7]. Measurements at higher temperatures were avoided to prevent intermixing and oxygen loss in the superlattice.

To summarize, in LSMO/LSFO superlattices with 6 unit cell thick sublayers FM LSMO exhibit a reduced magnetic ordering temperature of 200 K compared to the bulk value of 360 K while the AFM order in LSFO layers persists up to 400 K. Our experiments clearly show that when the magnetization of the LSMO layer is aligned with a magnetic field, a torque is created on the Fe moments in the LSFO layer through exchange coupling at the interface realigning the Fe moments as well. Through comparison with theoretical calculations we concluded that independent of the LSMO magnetization direction in the (001) plane, the Fe moments are always oriented perpendicular to the Mn moments. This perpendicular alignment is due to the frustrated exchange coupling at the interface and the weak anisotropy in the thin LSFO layer.

Research at the Center for Nanophase Materials Sciences and the Advanced Light Source were sponsored by Office of Basic Energy Sciences, U.S. Department of Energy.

[1] C. A. Chang, J. Appl. Phys. **68**, 4873 (1990).

[2] H. A. Dürr, G. Y. Guo, G. van der Laan, G. L. J. Lee, and J. A. C. Bland, Science **277**, 213 (1997).

[3] H. Ohldag, A. Scholl, F. Nolting, E. Arenholz, S. Maat, A. T. Young, M. Carey, and J. Stohr, Phys. Rev. Lett. **91**, 017203 (2003).

[4] M. D. Stiles and R. D. McMichael, Phys. Rev. B **59**, 3722 (1999).

[5] S. Maat, K. Takano, S. S. P. Parkin, and E. E. Fullerton, Phys. Rev. Lett. **87**, 087202 (2001).

[6] Y. Konishi, Z. Fang, M. Izumi, T. Manako, M. Kasai, H. Kuwahara, M. Kawasaki, K. Terakura, and Y. Tokura, J. Phys. Soc. Jpn. **68**, 3790 (1999).

[7] U. Shimony and J. M. Knudsen, Phys. Rev. **144**, 361 (1966).

[8] Y. Takamura, unpublished.

[9] E. Arenholz and S. O. Prestemon, Rev. Sci. Instrum. **76**, 083908 (2005).

[10] S. Stadler, Y. U. Idzerda, Z. Chen, S. B. Ogale, and T. Venkatesan, J. Appl. Phys. **87**, 6767 (2000).

[11] E. Arenholz, G. van der Laan, R. V. Chopdekar, and Y. Suzuki, Phys. Rev. Lett. **98**, 197201 (2007).

[12] G. van der Laan and B. T. Thole, Phys. Rev. B **43**, 13401 (1991).

[13] T. C. Schulthess and W. H. Butler, Phys. Rev. Lett. **81**, 4516 (1998).

[14] C. A. F. Vaz, J. A. C. Bland, and G. Lauhoff, Rep. Prog. Phys **71**, 056501 (2008).

[15] E. Arenholz, G. van der Laan, and F. Nolting, Appl. Phys. Lett. **93**, 162506 (2008).

[16] G. van der Laan E. Arenholz, R. V. Chopdekar, and Y. Suzuki, Phys. Rev. B **77**, 064407 (2008).

[17] G. van der Laan, unpublished.

[18] Theoretical spectra were obtained from the electric-dipole allowed transitions between the ground state $3d^n$ and the final state $2p^5 3d^{n+1}$ in the presence of an effective exchange field $g\mu_{\rm B}H = -0.1$ eV. The ground and final state wave functions were calculated in intermediate coupling using Cowan's Hartree-Fock code with relativistic correction. The results were broadened by a Lorentzian line shape increasing from $\Gamma = 0.1$ to 0.15 eV for the L_3 structure and $\Gamma = 0.3$ to 0.35 eV for the L_2 structure to account for the intrinsic linewidth and a Gaussian of

$\sigma = 0.2$ eV for the instrumental broadening. We used $10Dq = 1.6$ eV giving a total symmetric ground state $^6A_1$. Covalency was included by reducing the Hartree-Fock values of the $3d$-$3d$ Coulomb interaction to 60%, while the Slater integrals for the $2p$-$3d$ interaction were scaled to 80%.

Figure Caption

FIG. 1: (Color online) Comparison of experimental Fe $L_{2,3}$ XA and XMLD spectra obtained at normal incidence from the LSMO/LSFO superlattice (black dots) at $T = 50$ K with atomic multiplet calculations (red lines). The experimental geometry is depicted in the inset of (a) indicating the linear polarization **E** (grey arrow) at an angle ϕ to the [100] axis (dashed line) and applied external fields **H** (black arrows) at ϕ and $\phi + 90°$, respectively. (a) XA spectrum. (b) XMLD spectra I_0 (upper spectrum) and I_{45} (lower spectrum) obtained for $\phi = 0°$ and $\phi = 45°$, respectively.

FIG. 2: (Color online) Temperature dependence of magnitude of the x-ray dichroism in the LSMO/LSFO superlattice. (a) Mn $L_{2,3}$ XMCD (black open symbols) and Fe $L_{2,3}$ XMLD (red solid symbols) by aligning the Mn magnetization in the (001) surface plane. The Mn XMCD signal is obtained in 30° grazing incidence with the magnetic field collinear to the x-ray beam while the Fe XMLD was measured as in Fig. 1 with $\phi = 0°$. (b) Fe $L_{2,3}$ linear dichroism observed in 30° grazing incidence as the difference of XA spectra measured with the polarization in the (001) surface plane and close to perpendicular to it (open circles) [geometry in inset Fig. 2(b)]. A magnetic field was applied parallel to the x-ray beam (blue solid symbols).

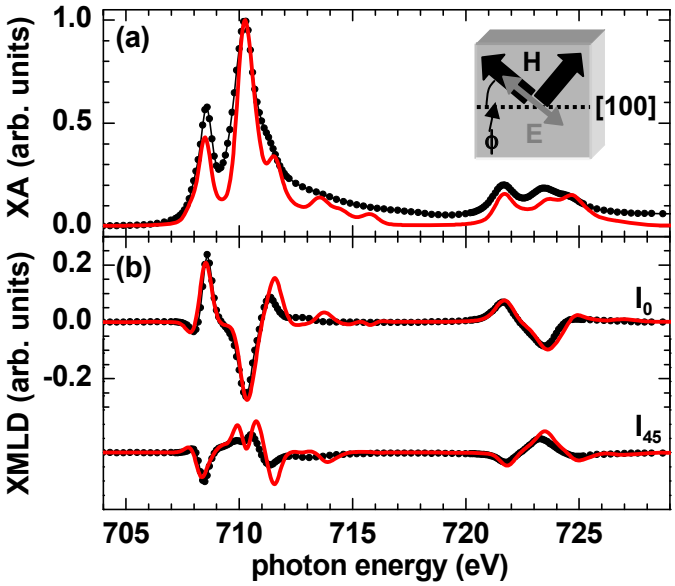
(a)
XA (arb. units)
1.0
0.5
0.0
H
[100]
E
ϕ
(b)
XMLD (arb. units)
0.2
0.0
-0.2
I0
I45
705
710
715
720
725
photon energy (eV)

Figure 1

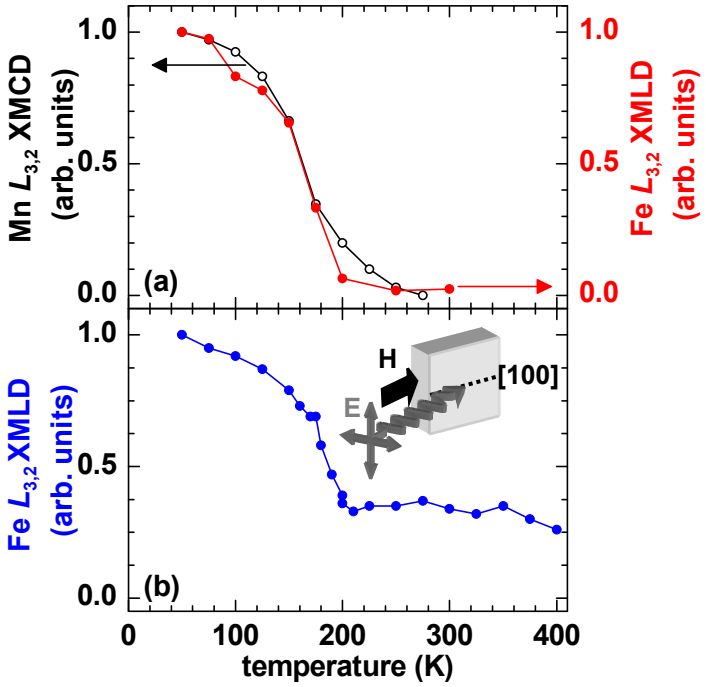
Mn $L_{3,2}$ XMCD (arb. units)
Fe $L_{3,2}$ XMLD (arb. units)
1.0
0.5
0.0
(a)
Fe $L_{3,2}$ XMLD (arb. units)
H
E
[100]
(b)
0
100
200
300
400
temperature (K)

Figure 2